1-Butene cracking to propene over P/HZSM-5: Effect of lanthanum

Nianhua Xue[a], Na Liu[a], Lei Nie[a], Yao Yu[b], Min Gu[b], Luming Peng[a], Xuefeng Guo[a], Weiping Ding[a,*]

[a] Lab of Mesoscopic Chemistry, Department of Chemistry, Nanjing University, Nanjing, Jiangsu Province 210093, China
[b] National Laboratory of Solid State Microstructures, Department of Physics, Nanjing University, Nanjing, Jiangsu Province 210093, China

ARTICLE INFO

ABSTRACT

HZSM-5 zeolite was modified using diammonium hydrogen phosphate and then lanthanum nitrate by impregnation. The surface structure and properties of P–La co-modified ZSM-5 were studied by the techniques of NH$_3$-TPD, D$_2$/OH isotopic exchange and solid state MAS NMR. In addition to modifying Brønsted acid sites (BAS) in HZSM-5, La additive also interacted with phosphorus species previously bonded to zeolitic hydroxyls or condensed in zeolite. Phosphorus species in zeolite surface were labile to form LaPO$_4$ entity when La was introduced to P/HZSM-5. Hence, some BAS were released which were previously bonded by phosphate. The 1-butene cracking was more dependent on the hydroxyl density, from the measurement of D$_2$/OH isotopic exchange, than the acidity of modified ZSM-5, evaluated from NH$_3$-TPD measurement. For the steamed catalysts, the highest activity was observed on the ZSM-5 co-modified by P and La, in which the number of P atoms surpassed that of lanthanum. Furthermore, the introduced lanthanum stabilized P species in the zeolite from leaching in steam at high temperatures.

© 2010 Elsevier B.V. All rights reserved.

1. Introduction

Propene is a versatile building block for important polymers, intermediates and chemicals. Its production is mainly from steam cracking and refineries. Alternative technologies have been also focused due to the greatly increasing demand for propene, such as propane dehydrogenation, olefin metathesis, methanol to olefins and low-value olefin cracking. The catalytic cracking of mixed C$_4$ olefins appears to be very attractive for researchers in the field recently. Looking through the work described in published literatures [1–14], it has been studied in detail on effective catalysts to optimal propene selectivity, e.g., pore size effect of different zeolite, aluminum distribution in zeolite and steam tolerance at high reaction temperatures. The 1-butene cracking reactions on acid catalysts include isomerization and dimerization by carbenium ion process, in which octenes are produced as intermediates for cracking products, e.g., propene, ethene and pentenes [15–19]. Butenes are also inclined to further oligomerization to by-products such as aromatic products and coke deposits on strong acid sites. Due to the coke formation easily poisons the active sites in zeolite catalysts during hydrocarbon transformation, it is a good method to add appropriate amount of steam in the feedstock against coke deposition [20], which, however, is harmful to the tetrahedrally coordinated and labile aluminum in the zeolite.

Up to now, many efforts have been made on the improvement of the hydrothermal stability of zeolite catalysts, especially for HZSM-5 [1,2,21–31]. Phosphorus modified HZSM-5 (P/HZSM-5) has shown attractive hydrothermal stability and the P/Al ratio in zeolite is important for the hydrothermal stability [27]. Our recent progress has further revealed that the enhanced hydrothermal stability by phosphorus doping is due to the formation of new acid sites during the steam treatment at high temperatures [1]. Besides phosphorous, lanthanum has also been proved effective in retarding the dealumination process [23,25,26] and is beneficial to reserve more Brønsted acid sites, from the hydrolysis of La^{3+}, in zeolitic cavities [32–38]. Although either lanthanum or phosphorus is beneficial to improve hydrothermal stability of HZSM-5, the effect of introducing La into P/HZSM-5 on the acidity and surface structure of the catalyst has not been elucidated in detail as well as butenes cracking performance. The present work reports the investigation on the doping effect of lanthanum in HZSM-5 and P/HZSM-5 with varied ratios of lanthanum to phosphorus, including the surface properties, hydrothermal stability of the catalysts as well as the catalytic performance for 1-butene cracking.

2. Experimental section

2.1. Materials

Phosphorus modified HZSM-5 (P/HZSM-5) catalysts were prepared as described previously [1]. HZSM-5 (Si/Al = 35, from Shanghai Research Institute of Petrochemical Technology) was impregnated with (NH$_4$)$_2$HPO$_4$ aqueous solution under stirring and

then was evaporated and calcined. P/HZSM-5 contained 0.9, 1.8 and 3 wt% of phosphorus contents and were named as 0.9P-Z, 1.8P-Z and 3P-Z, respectively.

Lanthanum was introduced to HZSM-5 and P/HZSM-5 by impregnation using La(NO$_3$)$_3$ aqueous solution. The slurry was stirred at room temperature for 1 h and then dried at 373 K overnight. The solid residue was calcined in air flow at 773 K for 3 h. The La modified HZSM-5 (La/HZSM-5) catalysts contained 4, 8, and 12 wt% lanthanum and were named as 4La-Z, 8La-Z and 12La-Z, respectively. The content of La in P/HZSM-5 was maintained constant (4 wt%), whereas the P loading was varied from 0.9, 1.8 to 3 wt%. They were named as La–0.9P-Z, La–1.8P-Z and La–3P-Z and corresponded to 1/1, 1/2, and 1/3.3 of La/P ratios in La–P/HZSM-5, respectively.

Steam treatment on the samples above mentioned was performed in 100% steam at 1073 K for 4 h as described in Ref. [1]. The steam treated samples were named according to the original catalysts with –S as postfix.

2.2. 1-Butene cracking

1-Butene (>99% purity) cracking was performed in a fixed-bed reactor with 10 mm inner diameter at atmospheric pressure. Catalysts were pretreated at 803 K for 1 h in 100 mL min^{-1} of air. Then a mixture of 1-butene and nitrogen (1-butene, WHSV = 13 h^{-1}, N$_2$/1-C$_4$H$_8$ = 3) was passed through the reactor at that temperature. The products were analyzed on-line in a gas chromatograph equipped with a PLOT Al$_2$O$_3$/Na$_2$SO$_4$ capillary column and a flame ionization detector (FID).

2.3. Characterization of catalysts

NH$_3$-TPD: Catalyst (100 mg) was activated at 873 K for 1 h in He flow (ultrahigh purity grade, 80 mL min^{-1}) and then cooled to 423 K before being exposed to ammonia. After adsorption of ammonia at 423 K for 1 h, the sample was flushed again in He for 1 h to remove physisorbed ammonia. Then the desorption profile was recorded by increasing the sample temperature from 423 to 873 K at a rate of 10 K min^{-1}. The signal of NH$_3$-TPD was recorded by TCD detector.

D$_2$/OH exchange: Concentrations of hydroxyls in prepared samples were determined by D$_2$/OH exchange technique as described in Ref. [1].

Porous texture and composition: The specific surface areas and pore volumes of the catalysts were determined by nitrogen adsorption measurement at 77 K on a Micrometrics ASAP 2020 instrument. Samples were treated at 623 K under vacuum before N$_2$ adsorption. Total surface area was calculated using the classical BET method and pore volume was evaluated by the *t*-plot method. Phosphorus contents in prepared catalysts were determined by X-ray fluorescence (XRF) using an ARL-9800 spectrometer.

Solid state MAS NMR: ^{31}P MAS NMR spectra were measured on a Bruker AV-300 solid state NMR spectrometer operating at a field of 7.0 T with a standard Bruker solid MAS probe. The pulse widths were 2.2 μs with 15 s repetition time and 2000 scans. Chemical shift was reported with respect to H$_3$PO$_4$. ^{27}Al MAS NMR spectra were recorded at 78.2 MHz with a spinning rate of 8 kHz and pulse widths of 0.5 μs with a 1 s repetition time. ^{27}Al chemical shifts were reported relative to [Al^{3+}(H$_2$O)$_6$].

3. Results and discussion

3.1. La effect on acidity and hydrothermal stability of HZSM-5

The ammonia-TPD profiles of zeolite HZSM-5 and 4 wt% La/HZSM-5 (4La-Z) are shown in Fig. 1. Two well resolved peaks, centered at ∼505 and 695 K, were observed on both samples. The
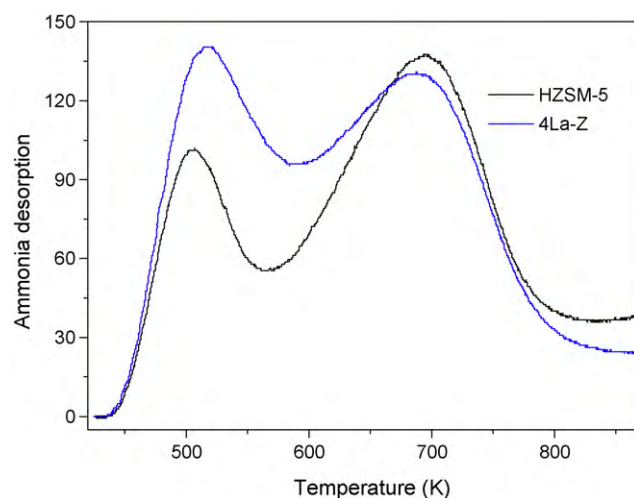

Fig. 1. NH$_3$-TPD profiles of HZSM-5 and 4La-Z (4 wt% La/HZSM-5).

peak in high temperature region was ascribed to the desorption of ammonia from strong acid sites. When HZSM-5 was loaded with 4% lanthanum (4La-Z), the amount of ammonia desorbed in high temperature region decreased to ca. 90%. The amount of weakly bound ammonia desorbed in the lower temperature region increased. When the lanthanum cation is loaded, there might be the weak Lewis acid sites to show the low temperature desorption peak. The positions of the both ammonia desorption peaks from HZSM-5 scarcely shifted by La modification.

To get insight into the status of La species in zeolite surface and the relationship between density of OH groups in zeolite surface and lanthanum modification, D$_2$/OH isotopic exchange was performed, which has been proved to be a precise method to detect the hydroxyl density in zeolite [1,39–42]. As shown in Fig. 2a, the hydroxyl density of HZSM-5 decreased to 867, 586 and 563 μmol g^{-1} of 4La-Z, 8La-Z and 12La-Z from 1020 μmol g^{-1} of HZSM-5. This reflected that introduced La^{3+} centers eliminated some bridging hydroxyls. Furthermore, hydroxyls in La/HZSM-5 appeared more readily to exchange with D$_2$ than those in the parent HZSM-5. The peak temperatures of HD evolution curves shifted to lower temperatures, showing the changes in environment of the hydroxyls in zeolite. For the steamed 4La-Z, from Fig. 2b, a little bit more hydroxyls were remained than in the steamed HZSM-5, showing the enhanced apparent hydrothermal stability by La addition.

From NH$_3$-TPD and D$_2$/OH results, it was deduced that adding La to zeolite HZSM-5 resulted in a decrease of the total amount of Brønsted acid sites in zeolite. This elimination was probably caused by the exchange of La^{3+} ion with bridged hydroxyls in zeolite, although some new acid sites might be generated by splitting the coordinated water molecules with La^{3+} ions [43]. The density of Brønsted acid sites in La/HZSM-5 decreased with the increase in La loadings. After steam treatment at high temperatures, more hydroxyls were detected in 4La-Z than HZSM-5, according to the D$_2$/OH exchange results, proving the promotive effect of La on the hydrothermal stability of the catalysts, although it was likely quite limited.

3.2. Phosphorus lability in P/HZSM-5 surface upon introducing lanthanum

Fig. 3a gives the NH$_3$-TPD profiles of modified zeolite. There were also two peaks of ammonia desorption observed on P/HZSM-5 catalysts (0.9P-Z, 1.8P-Z and 3P-Z), of which the densities of acid sites with ammonia desorption at higher temperatures decreased with increasing the phosphorus loadings. Doping 4 wt% La to 0.9P-Z resulted in the further decrease of strong acid sites in zeolite. The
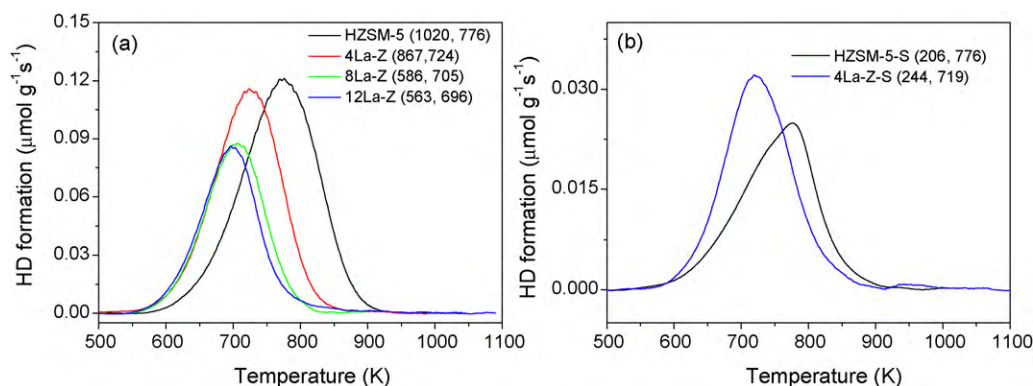
Fig. 2. D_2/OH isotopic exchange profiles of HZSM-5 and La modified HZSM-5. (a) Before steam treatment and (b) after steam treatment; values in parentheses represent the density of hydroxyl (μmol g^{-1}) measured by the D_2/OH exchange and the corresponding peak temperatures (K).

Fig. 3. (a) NH$_3$-TPD and (b) D_2/OH isotopic exchange profiles of P and La–P modified HZSM-5 (values in parentheses represent the density of hydroxyl (μmol g^{-1}) measured by the D_2/OH exchange and the corresponding peak temperatures (K)).
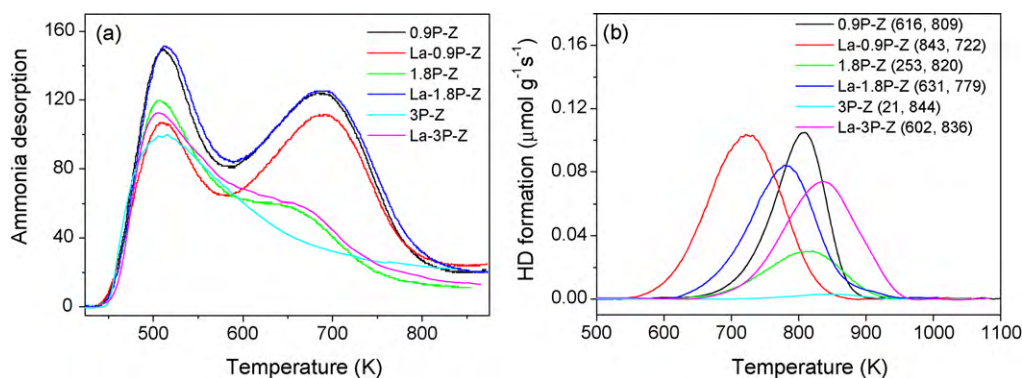
amount of ammonia adsorbed in the low temperature region also decreased at the same time. In terms of 1.8P-Z and 3P-Z, however, the amount of acid sites was greatly increased upon La introducing, indicating that some new acid sites were generated or some acid sites covered by phosphorus were restored again.

The D_2/OH isotopic exchange profiles of La doped P/HZSM-5 catalysts are shown in Fig. 3b. The density of hydroxyls in 1.8P-Z and 3P-Z increased with La doping, in line with the NH$_3$-TPD results. When 0.9P-Z was doped by La, however, an increase of density of hydroxyls was observed which was in contrast to the further decrease of acid sites from NH$_3$-TPD profiles. The difference among the three samples is significant in science to know the

surface structure of La–P/HZSM-5. The quantitative results of NH$_3$-TPD and D_2/OH exchange on all the catalysts are summarized in Table 1. As we know, in addition to enhanced hydrothermal stability caused by phosphorus modification, the interaction between phosphorus and zeolite also leads to decreased density and acid strength of Brønsted acid sites by P–OH groups replacing the bridging hydroxyls, whereas the interaction is not so strong against the elution with hot water [21] and phosphorus species also tend to lose in the steam cracking [1]. The phosphorus lability in zeolite surface should be noticed when further modification is carried out.

From NH$_3$-TPD and D_2/OH, acidity and hydroxyl density in P/HZSM-5 were not consistent with each other. About the result

Table 1
Acidity and hydroxyl density of P and La modified HZSM-5.

Sample	Acid site density from NH$_3$-TPD (μmol g^{-1})			OH groups density (μmol g^{-1})[a]
	Peak I (505 K)	Peak II (695 K)	Total acid sites	
HZSM-5	135	449	584	1020
4La-Z	248	405	652	867
0.9P-Z	221	394	615	616
La–0.9P-Z	160	363	523	843
1.8P-Z	205	157	362	253
La–1.8P-Z	223	403	626	631
3P-Z	109	55	164	21
La–3P-Z	230	208	438	602
0.9P-Z–S	108	192	299	438
La–0.9P-Z–S	66	117	183	258
1.8P-Z–S	93	105	198	154
La–1.8P-Z–S	84	146	229	412
3P-Z–S	95	54	149	113
La–3P-Z–S	80	105	185	285

[a] Detected by D_2/OH exchange.
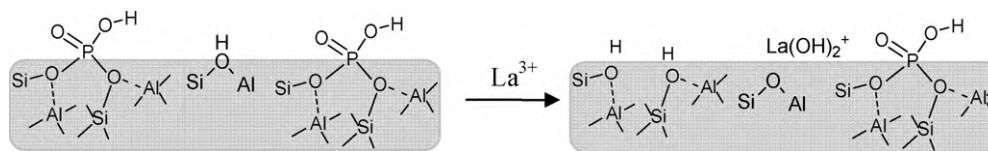
Scheme 1. Schematic show of the La ions that are introduced into the P/HZSM-5.

of NH$_3$-TPD, it gave the changes of acidity during introducing La to P/HZSM-5. D$_2$/OH determined the density of hydroxyls which could exchange with D$_2$ in solid surface. Surface properties of P/HZSM-5 containing 1.0 wt% P were different from the ones containing 2.0 wt% and 3.0 wt%. The former (1P-Z) contains grafted P–OH from phosphate and naked bridging OHs in zeolite which are not modified by phosphate. The surface of the latter samples (2P-Z and 3P-Z), however, is almost fully covered by P–OHs due to the excessive phosphorus. When La was introduced to 1P-Z, as shown in Scheme 1, lanthanum ions also exchange with the zeolitic protons to generate La–OH groups besides interacting with grafted P–OHs. However, lanthanum ions only interacted with surface P–OHs to release some bridging OH groups in 2P-Z and 3P-Z for the high P contents in zeolite surface. This can explain well why a decrease of the amount of desorbed ammonia but an increase of the density of hydroxyls is detected from 1P-Z to La–1P-Z.
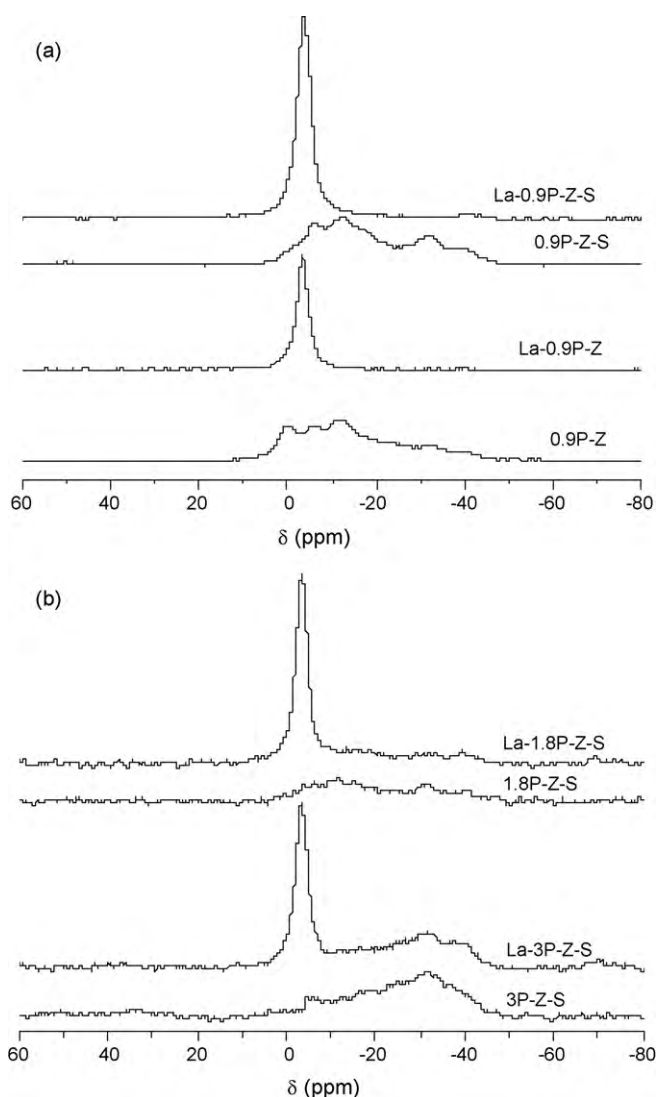
The previous work [1] has described the phosphorus state in P/HZSM-5 surface in detail. From ^{31}P MAS NMR spectra, shown in Fig. 4, P/HZSM-5 presented broad resonances in the range of 0–50 ppm which were related to mono-, condensed phosphorus species. After doping La to P/HZSM-5, an intense resonance at ca. −3.4 ppm emerged which was corresponded to the ^{31}P sites neighboring the residual water molecule contained in the LaPO$_4$ hexagonal structure [44]. This proved that the lanthanum was inclined to interact with the phosphorus bonded to the zeolitic hydroxyls to form LaPO$_4$. For the sample of 0.9P-Z, majority of phosphorous species became lanthanum phosphate as well as in steamed 0.9P-Z (0.9P-Z-S). While a part of phosphorous, besides lanthanum phosphate, still interacted with the zeolite framework of La–1.8P-Z and La–3P-Z (Fig. 4b). Hence, the resonance signaled in the range of 0 to −50 ppm was also observed in form of monomeric and condensed phosphorus species. This verified in turn phosphorus lability in P/HZSM-5 surface upon further modification by lanthanum dopant.

The ^{27}Al MAS NMR measurements were performed to check the chemical status of aluminum species and the results are depicted in Fig. 5. The introduction of 0.9 wt% phosphorus into HZSM-5 led to a decrease in tetrahedral framework Al (54 ppm) and to form intermediate Al species [1]. The octahedral Al species (0 to −14 ppm) were mainly due to distorted aluminum in framework upon phosphorus modification. When 4 wt% of lanthanum was introduced to 0.9P-Z (to be La–0.9P-Z), the intensity of the signal (54 ppm) of framework aluminum sharply increased. Simultaneously, the signals of the broad band at ca. 36 ppm vanished, which were attributed to tetrahedral aluminum in a distorted environment at either framework [45] or non-framework [46–48] positions. The species signaled in the range from 0 to −14 ppm also disappeared. These results revealed that the introduced lanthanum interacted with the pre-introduced phosphorus to release the tetrahedral aluminum sites from the distorted ones bonded to phosphorus. Little difference was distinguished from the NMR spectra of their steamed samples.
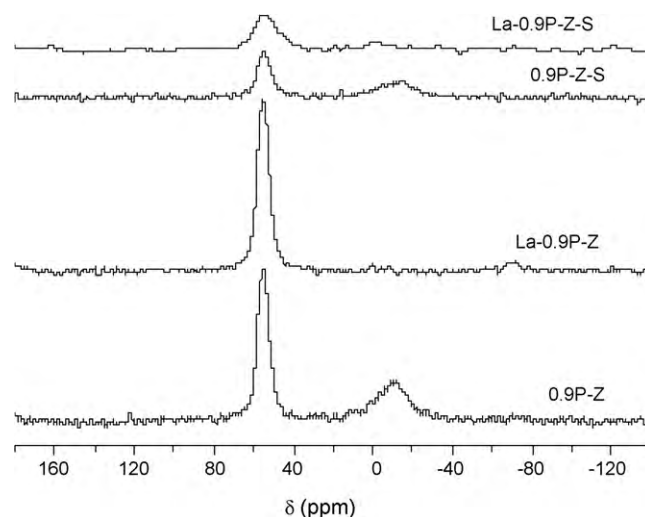

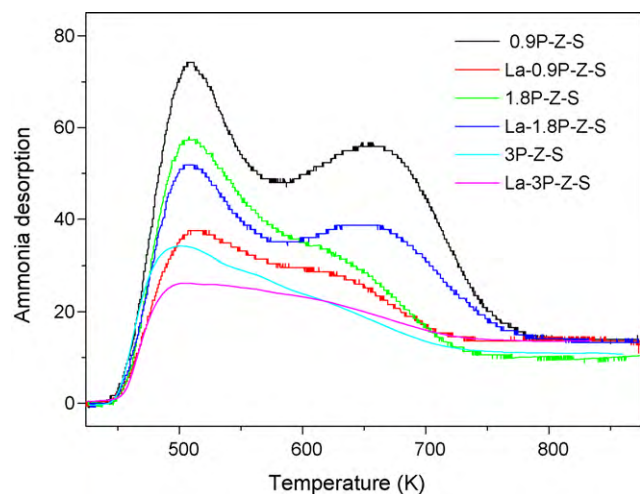**Fig. 4.** ^{31}P MAS NMR spectra of P and La modified HZSM-5.

Fig. 5. ^{27}Al MAS NMR spectra of P and La modified HZSM-5.

Fig. 6. NH$_3$-TPD profiles of steamed P and La–P modified HZSM-5.

Fig. 8. The D$_2$/OH exchange profiles of La(OH)$_3$–La$_2$O$_3$ and HZSM-5.

3.3. Further enhanced hydrothermal stability of P/HZSM-5 by doping La

To some extent, the amount of acid sites remained in steamed samples could reflect their hydrothermal stability. The results of NH$_3$-TPD (Fig. 6) and D$_2$/OH exchange (Fig. 7) revealed the changes of the hydrothermal stability of zeolites resulted from La and P modification. The pre-introduced phosphorus led to the specific decrease in strength and density of Brønsted acid sites and simultaneously improved the hydrothermal stability of HZSM-5. La–0.9P-Z showed poorer stability during steam treatment comparing with 0.9P-Z. This should be ascribed to reduced phosphorus content in P/HZSM-5 surface which was an effective element for hydrothermal stability of zeolite. Although lanthanum could enhance hydrothermal stability of zeolite to some extent, insufficient phosphorus in zeolite surface resulted in the poorer stability of La–0.9P-Z than 0.9P-Z. La–1.8P-Z and La–3P-Z presented further enhanced hydrothermal stability, when compared with their counterparts (1.8P-Z and 3P-Z, respectively). This was related to sufficient phosphorus in zeolite surface although some phosphorus species were consumed upon La doping. It can also be explained by the optimal P/Al ratio as ca. 0.5–0.7 for excellent hydrothermal stability of HZSM-5 [27].
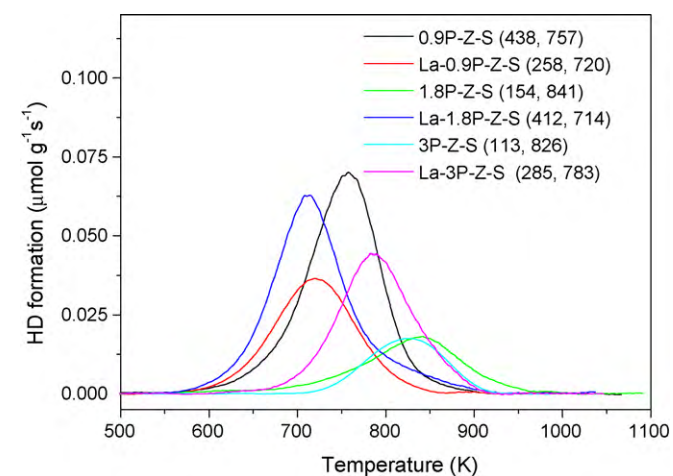

Fig. 7. D$_2$/OH isotopic exchange profiles of steamed P and La–P modified HZSM-5 (values in parentheses represent the density of hydroxyl (μmol g^{-1}) measured by the D$_2$/OH exchange and the corresponding peak temperatures (K)).
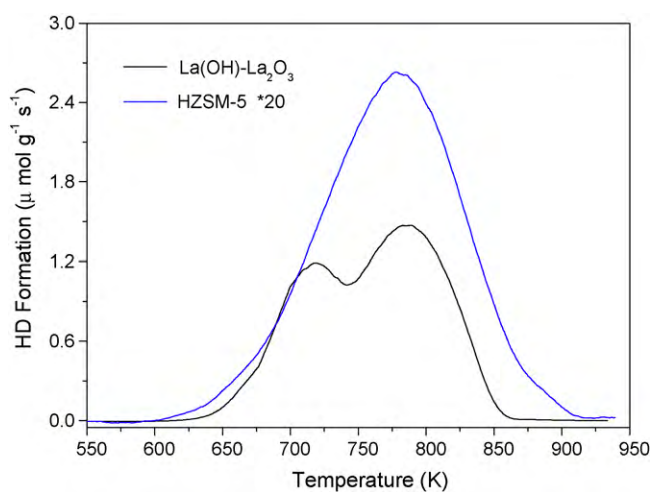
The introduction of La caused different effects on remained hydroxyl densities in steamed zeolites up to the P content introduced previously, owing to the La^{3+} ions could exchange with bridging hydroxyls and/or interact easily with P species to release some bridging hydroxyls and form LaPO$_4$ microcrystals. LaPO$_4$ formation eliminated the P–OH group and La ion exchange with zeolitic hydroxyls decreased density of Si(OH)Al in ZSM-5. But splitting of coordinated water molecules with La^{3+} ions generated some new hydroxyls. When the number of phosphorous was less than or equal to that of introduced lanthanum, as in La–0.9P-Z, the density of hydroxyls was determined by three effects: i.e., some La–OH, generated by the ion exchange of lanthanum ions with zeolite causing the increase of OH groups; P–OH groups, remained after being eliminated by the interaction between La ions and phosphorus species; and simultaneously released bridging OH groups. All hydroxyls in zeolite surface which could exchange with D$_2$ can be detected by D$_2$/OH exchange technique.

To check the exchange temperature of hydroxyls related to La–OH, the D$_2$/OH exchange experiments on La(OH)$_3$–La$_2$O$_3$ was performed. The result is presented in Fig. 8. The D$_2$/OH exchange technique could not distinguish the La–OH groups from zeolitic hydroxyls due to the overlapping of exchange temperature. Hence, detected density of in zeolite might include La–OH groups. This could give a good explanation about the decrease of strong acid sites from NH$_3$-TPD but increase of hydroxyl density from D$_2$/OH exchange in La modified 0.9P-Z. According to the results of present work, in terms of hydrothermal stability, phosphorus modification would be the preferable choice, and the lanthanum might be the second promoter, but less in amount than phosphorous.

3.4. Catalytic cracking of 1-butene on La and P modified HZSM-5

Catalytic cracking of 1-butene was performed on prepared catalysts. The 1-butene conversion and product distributions were obtained after 40 min of time on stream. The effect of La additive to HZSM-5 on catalytic conversion is shown in Fig. 9. Adding 4 wt% of La to HZSM-5 resulted in a decrease of 1-butene conversion owing to decreased concentration of Brønsted acid sites, for only minor changes of surface area and pore volume were detected (Table 2). Conversion of butenes decreased from 82.8% on HZSM-5 to 72.3% on 4La-Z and increasing the loading of La led to the further decrease in the butene conversion, as the performances observed on 8La-Z and 12La-Z. Table 3 gives the summary of product distribution and conversion of 1-butene cracking on modified zeolite catalysts and minor methane and ethane was omitted for clar-
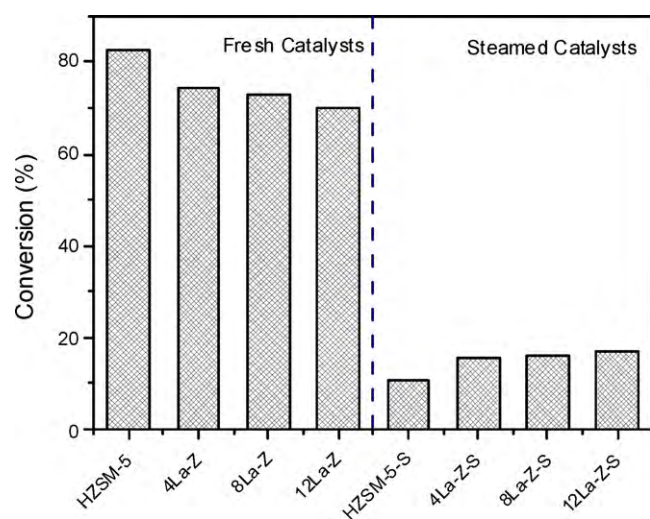
Fig. 9. Conversion of 1-butene over La/HZSM-5 catalysts at 803 K (N_2/butene = 3, 1 atm.).
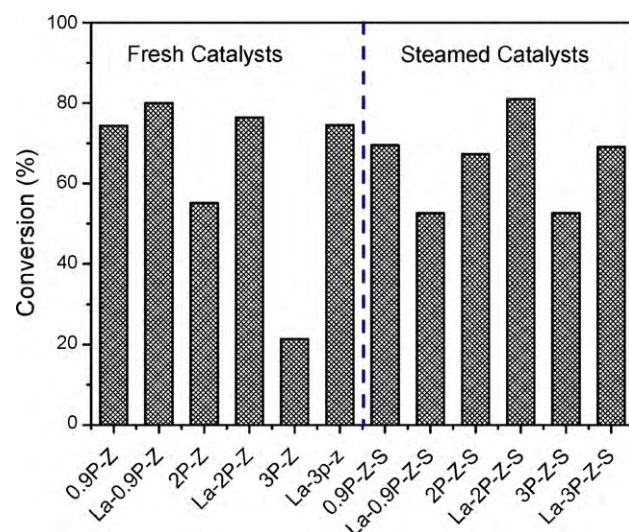

Fig. 10. Conversion of 1-butene over P and/or La modified HZSM-5 catalysts at 803 K (N_2/butene = 3, 1 atm.).

Table 2
Summary of surface areas and micropore volumes of modified zeolite HZSM-5.

Sample	BET surface area (m² g⁻¹)	Micropore volume (cm³ g⁻¹)
HZSM-5	389	0.120
4La-Z	372	0.116
4La-Z–S	314	0.101
HZSM-5–S	334	0.104
0.9P-Z	371	0.088
La–0.9P-Z	384	0.101
0.9P-Z–S	319	0.068
La–0.9P-Z–S	323	0.092
1.8P-Z	356	0.078
La–1.8P-Z	369	0.082
1.8P-Z–S	320	0.074
La–1.8P-Z–S	338	0.079
3P-Z	215	0.076
La–3P-Z	257	0.076
3P-Z–S	267	0.056
La–3P-Z–S	303	0.061

ity. Furthermore, introducing lanthanum to HZSM-5 enhanced the selectivity to propylene but decreased that to ethene. The decreased ethene/propylene ratio indicated that La/HZSM-5 catalyst is favorable to propylene production. The decreased selectivity of C_5^+ products was also observed as a consequence of decreased density of acid sites which were also responsible for oligomerization of olefins. The conversion of 1-butene on the steamed La/HZSM-5 catalysts is also represented in Fig. 9. Upon treatment in 100% steam at 1073 K for 4 h, HZSM-5 exhibited very low catalytic activity for 1-butene conversion due to serious dealumination. La/HZSM-5, however, showed a bit higher activity in comparison with HZSM-5, because of the partial resistance of dealumination by lanthanum doping [23].

In our previous work, the effect of phosphorus doping to HZSM-5 on the catalytic activity for 1-butene cracking was reported in detail [1]. The results of 1-butene reaction on P/HZSM-5 and La–P/HZSM-5 are shown in Fig. 10. Although the strong acid sites detected from NH_3-TPD results were reduced after adding La to 0.9P-Z, the 1-butene conversion increased. It revealed that 1-butene conversion was not simply proportional to the strong acid sites detected by NH_3-TPD and the less strong or weaker acid sites also made sense,

Table 3
Product distribution (wt%) of 1-butene cracking over P and La modified HZSM-5 catalysts at 803 K (N_2/butene = 3, 1 atm.).

Samples	Ethene yield (%)[a]	Propane yield (%)[a]	Propylene yield (%)[a]	Isobutane yield (%)[a]	n-Butane yield (%)[a]	C_5^+ yield (%)[a]	$C_4^=$ conv. (%)[a]
HZSM-5	8.8	2.0	33.4	2.4	2.1	36.7	85.8
4La-Z	8.5	1.7	34.1	2.6	2.0	25.3	74.3
8La-Z	7.1	1.7	33.8	2.4	2.0	25.5	72.6
12La-Z	6.7	1.1	33.7	2.1	1.8	24.6	70.0
HZSM-5–S	0.1	0	3.6	0.1	0.7	8.5	13.1
4La-Z–S	0.1	0	4.6	0.1	0.7	10.1	15.6
8La-Z–S	0.2	0	5.0	0.2	0.7	9.9	16.0
12La-Z–S	0.2	0	5.4	0.2	0.7	10.7	17.1
0.9P-Z	8.8	1.8	34.3	2.0	1.9	25.4	74.3
La–0.9P-Z	10.4	2.6	32.3	2.4	2.3	29.8	80.0
1.8P-Z	3.3	0.3	26.2	1.0	1.3	22.9	55.1
La–1.8P-Z	9.2	2.1	33.6	2.4	2.1	26.9	76.4
3P-Z	0.2	0	4.6	0.2	0.4	16.0	21.4
La–3P-Z	6.5	1.2	29.7	1.7	1.7	33.7	74.5
0.9P-Z–S	7.1	1.3	36.2	1.7	2.0	21.1	69.5
La–0.9P-Z–S	2.3	0.24	24.1	0.8	1.6	23.4	52.6
1.8P-Z–S	4.4	0.7	30.3	1.3	1.7	28.9	67.3
La–1.8P-Z–S	10.2	2.7	29.9	2.4	2.5	33.2	81.0
3P-Z–S	2.3	0.2	24.1	0.8	1.6	23.4	52.6
La–3P-Z–S	6.1	1.0	35.0	1.6	1.9	23.3	69.1

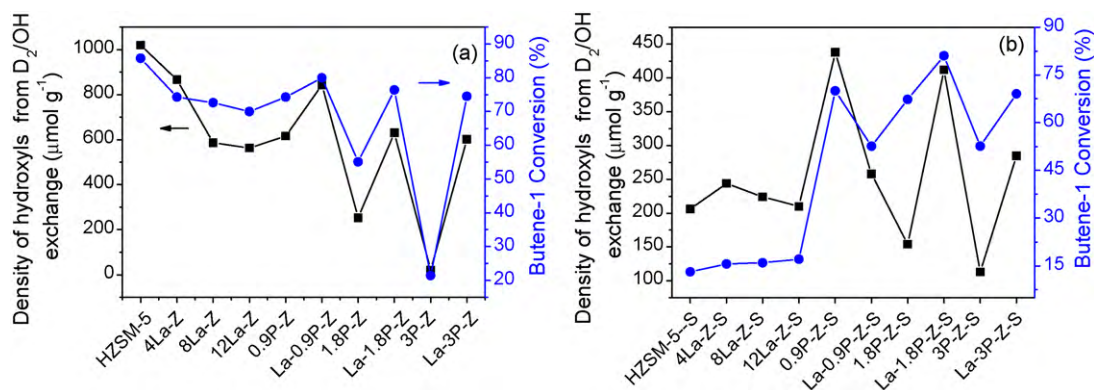[a] All the data were obtained at 40 min on stream.

Fig. 11. The relationship between the density of hydroxyls in modified zeolite (HZSM-5) and the conversion of butene. (a) Before steam treatment and (b) after steam treatment.

i.e., it would be better to correlate the 1-butene conversion with density of hydroxyl detected by D_2/OH exchange. For La–1.8P-Z and La–3P-Z, however, the number of La was less than that of P and interaction between La and P could not consume up the P species in zeolite surface as $LaPO_4$, while the majority of La itself was consumed as $LaPO_4$ and exchanged ions. Increases of hydroxyls and acid sites detected by D_2/OH exchange and NH_3-TPD were mainly due to the release of some zeolitic hydroxyls which were previously bonded to phosphorus species and some P–OH generated from condensed form. The $LaPO_4$ microcrystals in the zeolite channels would compensate the tension of zeolitic crystals and beneficial to the stability. The process is described as Scheme 1. Increased 1-butene cracking activity was observed on the La–1.8P-Z and La–3P-Z comparing with 1.8P-Z and 3P-Z, which were consistent with the hydroxyl density mentioned above.

Steamed La–0.9P-Z exhibited poor performance when compared with steamed 0.9P-Z. Contrarily, steamed La–1.8P-Z and La–3P-Z exhibited better catalytic performance when compared with their counterparts without La. The different effect of lanthanum on hydrothermal stability of P/HZSM-5 should be ascribed to different surface structures of obtained La–P/HZSM-5 catalysts with varied La/P ratios, as discussed in Section 3.3. In current work, it was amazingly observed that the steamed La–1.8P-Z (La–1.8P-Z–S) showed much better performance for the 1-butene cracking to propylene, even than that on 0.9P-Z–S, which is a promising catalyst for 1-butene cracking to propylene with excellent hydrothermal stability.

It seems that the conversion of 1-butene is quite consistent with the density of hydroxyls detected by D_2/OH exchange technique in prepared catalysts (as shown in Fig. 11). Then it comes to the conclusion that the hydroxyls in La–P/HZSM-5 surface are not entirely the strong acid sites but weak ones are active for 1-butene conversion. Our previous work has proved that the doped phosphorus in HZSM-5 is susceptible to lose under the steam at high temperatures [1]. By adding La to P/HZSM-5, almost no decrease in phosphorus content was found in La–P/HZSM-5 during the steam treatment process through the results of XRF analysis listed in Table 4, even for the La–1.8P-Z and La–3P-Z samples with excessive phosphorus species. This implied that lanthanum additives reacted with those phosphorus species which were not directly interact with zeolite. And those remained in zeolite in surface were interacting with zeolite tightly and not easy to lose in steam treatment. The current work has important implications in the preparation of stable catalysts for 1-butene cracking to propylene. Although phosphorus has been proved to be the efficient element for stability of HZSM-5 in steam, lanthanum additive is also important to further improve the stability including phosphorus lability. The excellent activity and stability of P–La/HZSM-5 cata-

Table 4
The P content in La and P modified HZSM-5 determined by XRF.

Sample	P content (wt%)	P lost (%)
0.9P-Z	0.72	–
0.9P-Z–S	0.68	4.6
La–0.9P-Z	0.72	–
La–0.9P-Z–S	0.74	–
1.8P-Z	1.68	–
1.8P-Z–S	1.54	8.3
La–1.8P-Z	1.68	–
La–1.8P-Z–S	1.69	–
3P-Z	2.71	–
3P-Z–S	2.58	9.5
La–3P-Z	2.73	–
La–3P-Z–S	2.78	–

lysts depends on appropriate phosphorus content and lanthanum additive.

4. Conclusions

Lanthanum was proved to enhance the hydrothermal stability of HZSM-5 to some extent. Introducing lanthanum to P/HZSM-5 led to phosphorus lability to form $LaPO_4$ clusters in zeolite channel. But the hydrothermal stability of zeolite HZSM-5 could be further enhanced by adding lanthanum to P/HZSM-5 when phosphorus amount was more than that of lanthanum. The further enhancement might be assigned to the synergistic effect of phosphorus and the formed $LaPO_4$ species in zeolite channel. The enhancing effect of phosphorus was dominant in La–P co-modified HZSM-5 and the La species in La–P/HZSM-5 significantly prohibit the phosphorus losing from the zeolite surface in steam at high temperatures.

References

[1] N. Xue, X. Chen, L. Nie, X. Guo, W. Ding, Y. Chen, M. Gu, Z. Xie, J. Catal. 248 (2007) 20–28.
[2] G. Zhao, J. Teng, Z. Xie, W. Jin, W. Yang, Q. Chen, Y. Tang, J. Catal. 248 (2007) 29–37.
[3] Y. Lu, M. He, X. Shu, B. Zong, Appl. Catal. A 255 (2003) 345–347.
[4] B. Wang, Q. Gao, J. Gao, D. Ji, X. Wang, J. Suo, Appl. Catal. A 274 (2004) 167–172.
[5] X. Zhu, S. Liu, Y. Song, L. Xu, Appl. Catal. A 288 (2004) 134–142.
[6] X. Zhu, S. Liu, Y. Song, S. Xie, L. Xu, Appl. Catal. A 290 (2005) 191–199.
[7] X. Zhu, S. Liu, Y. Song, L. Xu, Catal. Lett. 103 (2005) 201–210.

[8] G. Zhao, J. Teng, Y. Zhang, Z. Xie, Y. Yue, Q. Chen, Y. Tang, Appl. Catal. A 299 (2006) 167–174.
[9] G. Zhao, J. Teng, Z. Xie, W. Yang, Q. Chen, Y. Tang, Stud. Surf. Sci. Catal. 170B (2007) 1307–1312.
[10] J.C. Bricker, J.E. Rekoske, B. Glover, Stud. Surf. Sci. Catal. 172 (2007) 49–54.
[11] P. Sazama, J. Dedecek, V. Gabova, B. Wichterlova, G. Spoto, S. Bordiga, J. Catal. 254 (2008) 180–189.
[12] X. Tang, H. Zhou, W. Qian, D. Wang, Y. Jin, F. Wei, Catal. Lett. 125 (2008) 380–385.
[13] G. Xu, X. Zhu, X. Niu, S. Liu, S. Xie, X. Li, L. Xu, Micropor. Mesopor. Mater. 118 (2009) 44–51.
[14] G. Xu, X. Zhu, S. Xie, X. Li, S. Liu, L. Xu, Catal. Lett. 130 (2009) 204–210.
[15] M. Guisnet, P. Andy, N.S. Gnep, E. Benazzi, C. Travers, J. Catal. 158 (1996) 551–560.
[16] P. Mériaudeau, R. Bacaud, L. Ngoc Hung, A.T. Vu, J. Mol. Catal. A 110 (1996) L177–L179.
[17] C. Pazè, B. Sazak, A. Zecchina, J. Dwyer, J. Phys. Chem. B 103 (1999) 9978–9986.
[18] O. Bortnovsky, P. Sazama, B. Wichterlova, Appl. Catal. A 287 (2005) 203–213.
[19] J. Houzvicka, R. Klik, L. Kubelkova, V. Ponec, Appl. Catal. A 150 (1997) 101–114.
[20] S. Liu, R. Ohnishi, M. Ichikawa, J. Catal. 220 (2003) 57–65.
[21] G. Lischke, R. Eckelt, H.G. Jerschkewitz, B. Parlitz, E. Schreier, W. Storek, B. Zibrowius, G. Ohlmann, J. Catal. 132 (1991) 229–243.
[22] G. Ohlmann, H.G. Jerschkewitz, G. Lischke, R. Eckelt, B. Parlitz, E. Schreier, B. Zibrowius, E. Loeffler, Stud. Surf. Sci. Catal. 65 (1991) 1–20.
[23] J. Zhuang, D. Ma, G. Yang, Z. Yan, X. Liu, X. Liu, X. Han, X. Bao, P. Xie, Z. Liu, J. Catal. 228 (2004) 234–242.
[24] G. Yang, J. Zhuang, Y. Wang, D. Zhou, M. Yang, X. Liu, X. Han, X. Bao, J. Mol. Struct. 737 (2005) 271–276.
[25] G. Yang, Y. Wang, D. Zhou, X. Liu, X. Han, X. Bao, J. Mol. Catal. A 237 (2005) 36–44.
[26] G. Yang, Y. Wang, D. Zhou, J. Zhuang, X. Liu, X. Liu, X. Bao, J. Chem. Phys. 119 (2003) 9765–9770.
[27] T. Blasco, A. Corma, J. Martínez-Triguero, J. Catal. 237 (2006) 267–277.
[28] G. Caeiro, P. Magnoux, J.M. Lopes, F. Ramoa Ribeiro, S.M.C. Menezes, A.F. Costa, H.S. Cerqueira, Appl. Catal. A 314 (2006) 160–171.
[29] K. Damodaran, J.W. Wiench, S.M. Cabral de Menezes, Y.L. Lam, J. Trebosc, J.P. Amoureux, M. Pruski, Micropor. Mesopor. Mater. 95 (2006) 296–305.
[30] J.A.Z. Pieterse, G.D. Pirngruber, J.A. van Bokhoven, S. Booneveld, Stud. Surf. Sci. Catal. 170B (2007) 1386–1391.
[31] B. Ding, S. Huang, W. Wang, THEOCHEM 851 (2008) 207–212.
[32] A.V. Inanow, G.W. Graham, M. Shelef, Appl. Catal. B 21 (1999) 243–258.
[33] E.F.T. Lee, L.V.C. Rees, Zeolites 7 (1987) 143–147.
[34] E.F.T. Lee, L.V.C. Rees, Zeolites 7 (1987) 545–548.
[35] C. Gauthier, B. Chiche, A. Finiels, P. Geneste, J. Mol. Catal. 50 (1989) 219–229.
[36] R. Carvajal, P.J. Chu, J.H. Lunsford, J. Catal. 125 (1990) 123–131.
[37] A. Martins, J.M. Silva, C. Henriques, F.R. Ribeiro, M.F. Ribeiro, Catal. Today 107–108 (2005) 663–670.
[38] J. Huang, Y. Jiang, V.R. Reddy Marthala, Y.S. Ooi, J. Weitkamp, M. Hunger, Micropor. Mesopor. Mater. 104 (2007) 129–136.
[39] J.A. Biscardi, G.D. Meitzner, E. Iglesia, J. Catal. 179 (1998) 192–202.
[40] W.P. Ding, G.D. Meitzner, D.O. Marler, E. Iglesia, J. Phys. Chem. B 105 (2001) 3928–3936.
[41] W.P. Ding, S.Z. Li, G.D. Meitzner, E. Iglesia, J. Phys. Chem. B 105 (2001) 506–513.
[42] W.P. Ding, G.D. Meitzner, E. Iglesia, J. Catal. 206 (2002) 14–22.
[43] P. Tynjala, T.T. Pakkanen, J. Mol. Catal. A 110 (1996) 153–161.
[44] B. Glorieux, M. Matecki, F. Fayon, J.P. Coutures, S. Palau, A. Douy, G. Peraudeau, J. Nucl. Mater. 326 (2004) 156–162.
[45] Z. Yan, D. Ma, J. Zhuang, X. Liu, X. Liu, X. Han, X. Bao, F. Chang, L. Xu, Z. Liu, J. Mol. Catal. A 194 (2003) 153–167.
[46] J.X. Chen, T.H. Chen, N.J. Guan, J.Z. Wang, Catal. Today 93–95 (2004) 627–630.
[47] S.M.C. Menezes, V.L. Camorim, Y.L. Lam, R.A.S. San Gil, A. Bailly, J.P. Amoureux, Appl. Catal. A 207 (2001) 367–377.
[48] T.H. Chen, B.H. Wouters, P.J. Grobet, Eur. J. Inorg. Chem. 2 (2000) 281–285.